An RNA G-Quadruplex Structure within the ADAR 5'UTR Interacts with DHX36 Helicase to Regulate Translation

Lyu, Kaixin; Chen, Shuo-Bin; Chow, Eugene Yui-Ching; Zhao, Haizhou; Yuan, Jia-Hao; Cai, Meng; Shi, Jiahai; Chan, Ting-Fung; Tan, Jia-Heng; Kwok, Chun Kit

Published in:
Angewandte Chemie (International Edition)

Published: 23/12/2022

Document Version:
Post-print, also known as Accepted Author Manuscript, Peer-reviewed or Author Final version

Published version (DOI):
10.1002/anie.202203553

Publication details:
Lyu, K., Chen, S.-B., Chow, E. Y.-C., Zhao, H., Yuan, J.-H., Cai, M., Shi, J., Chan, T.-F., Tan, J.-H., & Kwok, C. K. (2022). An RNA G-Quadruplex Structure within the ADAR 5'UTR Interacts with DHX36 Helicase to Regulate Translation. *Angewandte Chemie (International Edition)*, *61*(52), Article e202203553. https://doi.org/10.1002/anie.202203553

RESEARCH ARTICLE

An RNA G-Quadruplex Structure within the ADAR 5'UTR Interacts with DHX36 Helicase to Regulate Translation

Kaixin Lyu, Shuo-Bin Chen, Eugene Yui-Ching Chow, Haizhou Zhao, Jia-Hao Yuan, Meng Cai, Jiahai Shi, Ting-Fung Chan, Jia-Heng Tan & Chun Kit Kwok*

[*] K. Lyu, H. Zhao, Prof. Dr. C. K. Kwok
Department of Chemistry and State Key Laboratory of Marine Pollution
City University of Hong Kong
Hong Kong SAR, China
Email: ckkwok42@cityu.edu.hk
M. Cai, Prof. Dr. J. Shi, Prof. Dr. C. K. Kwok
Shenzhen Research Institute of City University of Hong Kong,
Shenzhen, China
Prof. Dr. S. B. Chen, J. H. Yuan, Prof. Dr. J. H. Tan
School of Pharmaceutical Sciences, Guangdong Provincial Key Laboratory of New Drug Design and Evaluation
Sun Yat-sen University
Guangzhou, 510006 China
E. Y. C. Chow, Prof. Dr. T. F. Chan
School of Life Sciences, and State Key Laboratory of Agrobiotechnology
The Chinese University of Hong Kong
Hong Kong SAR, China
M. Cai, Prof. Dr. J. Shi
Department of Biomedical Sciences, College of Veterinary Medicine and Life Sciences, Tung Biomedical Sciences Center
City University of Hong Kong
Hong Kong SAR, China
Prof. Dr. J. Shi
Department of Biochemistry, Synthetic Biology Translational Research Programmes, Yong Loo Lin School of Medicine
National University of Singapore
Singapore

Abstract: RNA G-quadruplex (rG4) structures in the 5' untranslated region (5'UTR) play crucial roles in fundamental cellular processes. ADAR is an important enzyme that binds to double-strand RNA and accounts for the conversion of Adenosine to Inosine in RNA editing. However, so far there is no report on the formation and regulatory role of rG4 on ADAR expression. Here, we identify and characterize a thermostable rG4 structure within the 5'UTR of the *ADAR1* mRNA and demonstrate its formation and inhibitory role on translation in reporter gene and native gene constructs. We reveal rG4-specific helicase DHX36 interacts with this rG4 *in vitro* and in cells under knockdown and knockout conditions by GTFH (G-quadruplex-triggered fluorogenic hybridization) probes and modulates translation in an rG4-dependent manner. Our results further substantiate the rG4 structure-DHX36 protein interaction in cells and highlight rG4 to be a key player in controlling *ADAR1* translation.

Introduction

RNA adopts various secondary structures to carry out its function in gene expression and regulation, and one of the well-studied secondary structures is RNA G-quadruplex (rG4).[1] Guanine-rich sequences on RNA can self-assemble into G-quartet through Hoogsteen hydrogen bonds (Figure. 1A), and several G-quartets can stack on each other to assemble an rG4 that is connected by loop nucleotides (Figure. 1B). [2] This thermodynamically stable structure, with a preference for sodium ion (Na^+) and potassium ion (K^+), but not lithium ion (Li^+), was reported to have functions in almost every biochemical process in cells, including transcription, RNA metabolism, and translation.[2b, 2c, 3] Over the years, studies have reported rG4 formation and its biological function in the 5' untranslated region (5'UTR) of messenger RNA (mRNA).[4] Schaeffer et al. first demonstrated the formation and repressive role of rG4 on translation in the 5'UTR of *FMR1* transcript in rabbit reticulocyte lysate and Kumari et al. first verified the translation inhibition role of *NRAS* proto-oncogene 5'UTR rG4 in cell-free translation system.[5] Later, several more studies have further supported the repressing role of 5'UTR rG4 on translation in both cell-free and cell-based reporter gene system in different organisms.[4a, 4b, 6] However, research gaps remain in direct corroboration on rG4 folding status in cells, rG4-mediated control on the protein expression, and whether other biomolecules such as proteins have a key role in the associated gene regulation.

rG4-binding proteins (rG4-BPs), such as FMRP, FUS, nucleolin, DDX21, and DHX36, recognize rG4s and control the rG4 folding dynamics in cells, which lead to regulation in RNA metabolism and translation.[7] Among all, DHX36, also known as RHAU and G4R1, exhibited high rG4 binding affinity and specificity.[8] DHX36 is a DEAH-box helicase that is ubiquitously expressed and indispensable for development and displays ATP-dependent folding on both rG4 and DNA G-quadruplex (dG4).[8-9] In 2008, Creacy et al. first demonstrated the high binding affinity and resolving enzymatic activity of DHX36 with rG4[10] and Sexton reported that the 5' guanosine tracts on human telomerase RNA (hTR) can be recognized by the N-terminal DHX36 domain.[11] In 2018, Chen et al. solved the co-crystal structure of DHX36 interaction with a dG4 and reported the folding of a DNA-binding-

induced α-helix on the N-terminal DHX36-specific motif (DSM).[7a] Besides studying the cellular role of DHX36 on reporter gene level, Sauer et al. demonstrated that the knockout of DHX36 led to an increase of mRNA abundance harboring rG4 in stress granules but did not directly affect the translation machinery.[12] In addition, studies have shown DHX36 specifically interacts with *Gnai2* mRNA on its 5'UTR rG4 in skeletal muscle stem cells to control native Gnai2 translation.[13] Moreover, DHX36 is critical for heart development through resolving *Nkx2-5* mRNA 5'UTR G4.[14] Nevertheless, the biochemical recognition and unwinding modulation of DHX36 towards rG4 has not yet been elucidated, especially the direct imaging evidence under microscope, as well as its impact on protein translation.

RNA editing is of considerable significance in gene modification, and in mammalian cells, almost 90% of RNA editing is the adenosine-to-inosine (A-to-I) conversion, catalyzed by ADAR (Adenosine Deaminase Acting on RNA).[15] The editing of adenosine to inosine in RNA could be interpreted as guanosine (G) by the translation machinery because of the similar chemical structure between I and G.[15c, 16] The ADAR A-to-I RNA editing may trigger translation frameshift and codon substitution in the open reading frame region, and affect alternative splicing, translation efficacy, miRNA processing, and RNA stability in UTRs.[15a, 17] Mammalian genomes contain 3 *ADAR* genes (*Adar1*, *Adar2*, *Adar3*), and encode 4 ADAR proteins: ADAR1p150, ADAR1p110, ADAR2, and ADAR3, which have distinct functions and localization in cells.[15b, 18] ADAR1 is responsible for the deamination reaction and ubiquitously expressed, and occurs in two protein isoforms, the longer isotype p150 and shorter isotype p110,[16, 19] with the contribution of each isoform to the editing landscape still unclear due to the co-expression of the two isoforms.[20]

Recently, Kwok et.al., developed rG4-seq, an *in vitro* rG4 profiling method that enables the mapping of rG4s in transcriptome.[21] Within the rG4-seq dataset, we uncovered a G-rich sequence in the 5'UTR of the human *ADAR1* p110 isoform. Motivated by this, we are interested to investigate the potential formation and function of rG4 in this transcript. In addition, considering the critical association between DHX36 and rG4 reported above, we devoted ourselves to demonstrating the direct evidence of helicase-rG4 recognition and uncovering the DHX36's role in gene translation through the regulation of rG4. In this work, we have first identified and characterized the formation of *ADAR1* 5'UTR rG4 *in vitro* and in cells. We then confirmed the DHX36-rG4 interaction through hybridized probe imaging in DHX36 KO (knockout) cells and revealed that DHX36 controls translation through the modulation of rG4.

Results and Discussion

To study the *ADAR* 5'UTR rG4 motif, we carried out spectroscopic assays on both *ADAR* 5'UTR rG4wt and rG4mut motif (Supplementary Table 1) under Li^+ (G4-non-stabilizing) and K^+ (G4-stabilizing) conditions (Supplementary Figure. 1 and Supplementary Figure. 2). Using circular dichroism (CD)-detected titration, we observed a positive peak at around 265 nm and a negative peak at around 240 nm for *ADAR* 5'UTR rG4wt motif, whereas with much weaker peaks for *ADAR* 5'UTR rG4mut motif, under K^+ condition (Supplementary Figure. 1). In addition, we found the CD profile pattern to be stronger when the Li^+ condition is replaced by K^+ condition for rG4wt motif, underscoring the formation of rG4 with parallel topology. We also conducted UV-detected melting and observed the hypochromic shift at 295 nm for the rG4wt motif, but not the rG4mut motif, with a melting temperature (T_m) to be above 82°C, indicating the rG4 is highly thermostable (Supplementary Figure. 2).

To examine the formation of *ADAR* 5'UTR rG4 with flanking sequences, we introduced the native sequence around both rG4wt and rG4mut motif and referred to them as *ADAR* 5'UTR rG4wt region and rG4mut region (Supplementary Table 1). G4-specific ligands such as Thioflavin T (ThT) and N-Methyl-mesoporphyrin IX (NMM) were used and the G4 ligand-enhanced fluorescence assays were performed. After normalizing the intrinsic fluorescence background of the ligands (NMM and ThT), strong fluorescence magnification was observed for both ligands on *ADAR* 5'UTR rG4wt region when comparing K^+ over Li^+ conditions, whereas little to no noticeable change was spotted for the *ADAR* 5'UTR rG4mut region (Figure. 1C-F). Together, these spectroscopic analyses demonstrated that the *ADAR* 5'UTR rG4 can be folded under physiological K^+ concentration, temperature, and native sequence context.

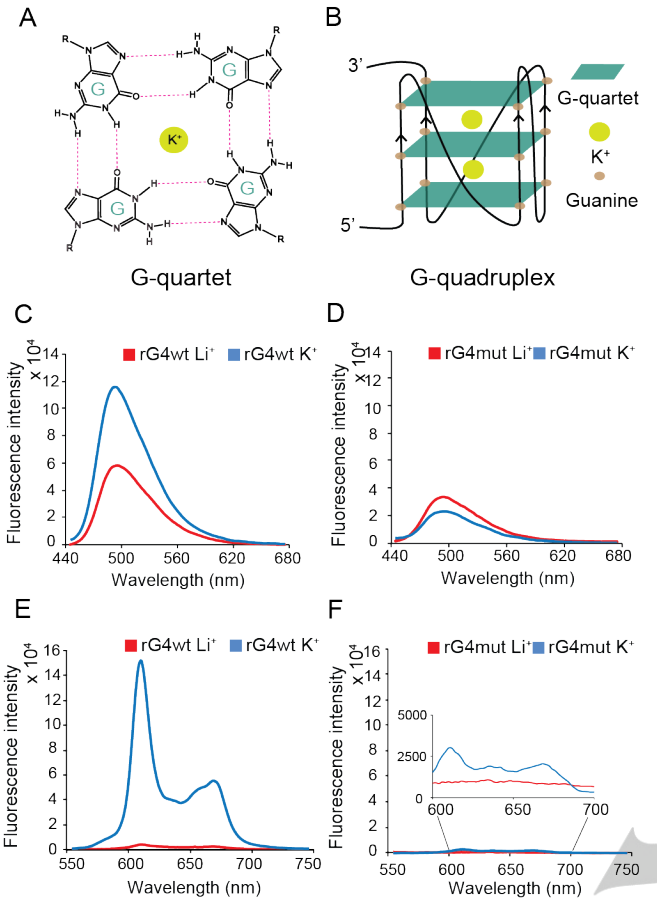

Figure 1. Fluorescence turn-on assay reveals rG4 motif formation in the *ADAR* 5'UTR. (A) G-quartet chemical structure stabilizing by potassium ion (K^+) presents in the center. (B) G-quadruplex structure is composed of G-quartets stacking together. (C)(D) ThT ligand-enhanced fluorescence on the (C) *ADAR* 5'UTR rG4wt region and (D) *ADAR* 5'UTR rG4mut region under 150 mM LiCl and KCl conditions, respectively. Spectra under KCl condition in (C) exhibited a positive 2-fold difference in fluorescence (at 494 nm), relative to the LiCl condition, while little difference was observed for (D), suggesting rG4 formation in *ADAR* 5'UTR rG4wt, rather than *ADAR* 5'UTR rG4mut region. (E)(F) NMM ligand-enhanced fluorescence on the (E) *ADAR* 5'UTR rG4wt region and (F) *ADAR* 5'UTR rG4mut region in 150 mM LiCl and KCl, respectively. Spectra under KCl condition in (E) showed a positive 34-fold difference in fluorescence (at 610 nm), relative to the LiCl condition, while only a small difference was observed for (F), indicating rG4 formation in *ADAR* 5'UTR rG4wt but not in *ADAR* 5'UTR rG4mut region. An inset is shown for the 600-700nm region for (F).

To further support rG4 formation, we performed reverse transcriptase stalling (RTS) assay on both *ADAR* 5'UTR rG4wt region and rG4mut region (Figure. 2A and Supplementary Figure. 3). The principle of this assay relies on the reverse transcriptase stalling mediated by the presence of thermostable rG4 structure, leading to truncated cDNA fragment that informs the location of rG4.[22] We observed a strong RTS band for the *ADAR* 5'UTR rG4wt region under K^+ condition near the 3' end of the rG4 motif, and its stalling intensity was determined to be approximately 3 times more intense than the Li^+ condition, indicating the formation of rG4 (Figure. 2A and Supplementary Table 2). We employed the same assay on *ADAR* 5'UTR rG4mut region as control, with no RTS band detected (Supplementary Figure. 3), supporting the stalling observed is caused by the rG4 structure. Moreover, we inspected and analyzed the recently reported rG4-seq high-throughput sequencing data(Supplementary Table 3)[21] and obtained the ratio of stalled reads (RSR) data (Supplementary Figure. 4). High RSR metric suggests a strong RTS effect and most positions with high RSR concentrate are at the last 2 G-tracts in the *ADAR* 5'UTR rG4wt region, which are largely consistent with the RTS stalling band patterns on the gel. Interestingly, a minor stalling was observed near the bottom of the gel under K^+ condition (Figure. 2A, lane 1). Considering there was no such pattern under the Li^+ condition (Figure. 2A, lane 2) and *ADAR* 5'UTR rG4mut at the same probing region (Supplementary Figure. 3), we reasoned that these few guanines may be involved in the formation of an rG4 motif with a long loop, albeit at a lower population as compared to the main rG4 motif mentioned earlier. Together these findings disclosed the formation and location of the rG4 in the *ADAR* 5'UTR rG4wt region and provided support to the spectroscopic data presented above.

To further characterize *ADAR* 5'UTR rG4 structure feature, we also employed another assay, selective hydroxyl acylation analyzed by lithium-ion mediated primer extension (SHALiPE)[23] on both *ADAR* 5'UTR rG4wt region and rG4mut region (Figure. 2B and Supplementary Figure. 5). 2-methylnicotinic acid imidazolide (NAI) can react with flexible nucleotides at the 2'hydroxyl position of RNA to form 2'O-adduct. The adduct can cause reverse transcription halting and shorten cDNA fragment, which reports the NAI-modified site in RNA at nucleotide resolution.[23] From the data, we observed that for the rG4wt region, while most of the NAI-modified nucleotides are of similar pattern between the Li^+ and K^+ conditions, the modified nucleotides pattern near the rG4 motif region are markedly different under Li^+ and K^+ conditions (Figure. 2B, blue box), verifying a local change in RNA structural conformation between the conditions. As a negative control, we conducted an identical assay on the *ADAR* 5'UTR rG4mut region, and no observable difference was detected in the NAI modification patterns between the 2 conditions (Supplementary Figure. 5), highlighting that the local structural change observed in the rG4wt region is due to rG4 formation under K^+ condition. To demonstrate that the *ADAR* 5'UTR rG4 can form under physiological-relevant condition, we carried out SHALiPE assay on the rG4wt region construct in cell lysate (Supplementary Figure. 6) and discovered that the NAI modification pattern of rG4wt region is remarkably consistent with that under K^+ condition rather than Li^+ condition *in vitro* (Figure. 2B and Supplementary Figure. 5). Collectively, our structural analysis provides strong confirmation on the formation of *ADAR* 5'UTR rG4 conformation both *in vitro* and in cell lysate.

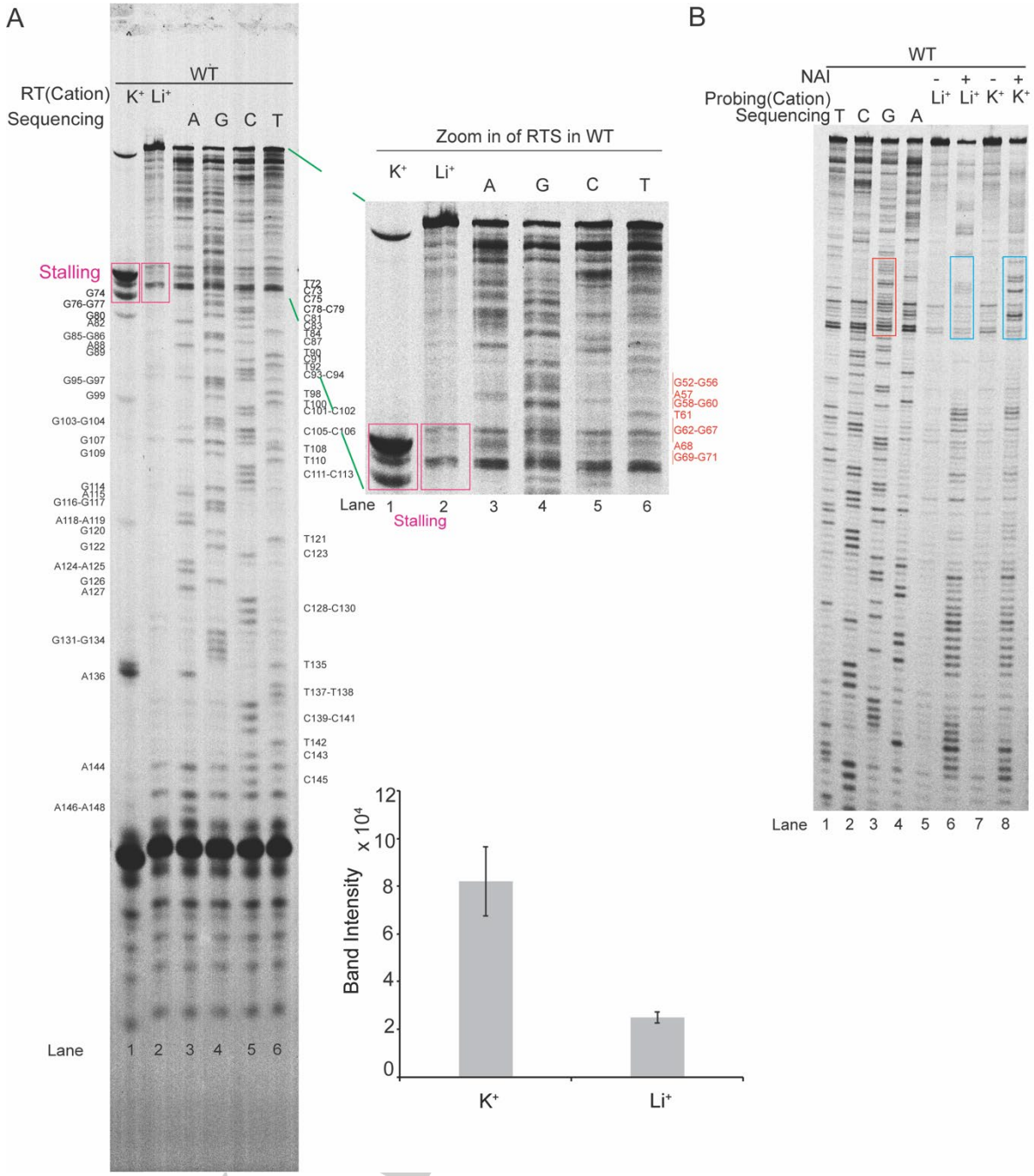

Figure 2. RNA structure probing assay on *ADAR* 5'UTR rG4wt region reports rG4 formation *in vitro*. (A) RTS on *ADAR* 5'UTR rG4wt region. On the right is the zoom-in of the rG4 motif region (pink box) from the RTS gel. The Gs in red is the four G-tracts from the *ADAR* 5'UTR rG4wt region. In lane 1 and 2, 150 mM K^+ and 150 mM Li^+, respectively, were used for reverse transcription. Lanes 3-6 are ladders generated by dideoxynucleotide sequencing. The stalling sites were near the 3' end of the G-rich sequence, i.e., the last 2 G-tracts. The rG4 is stable even in the presence of Li^+, therefore RTS was also observed in Li^+, and dideoxynucleotide lanes as well. The quantification of stalling band intensity is shown in the graph below. The band intensity under K^+ is about 3 times higher than Li^+, supporting rG4 formation. Data from two replicates were used. (B) SHALiPE on *ADAR* 5'UTR rG4wt region. RNAs were incubated with DMSO (control) or NAI under Li^+ and K^+ (lanes 5-8). Lanes 1-4 are dideoxynucleotide sequencing lanes. The rG4 at the *ADAR* 5'UTR rG4wt region displayed markedly different NAI profiles between Li^+ and K^+ conditions (lanes 6 and 8, labeled in a blue box). Due to the many G nucleotides in the *ADAR* 5'UTR rG4wt motif (red box), multiple rG4 conformations are likely formed.

To investigate the folding status of *ADAR* 5'UTR rG4 in cells, we visualized its formation in HEK293T cells by transfecting *ADAR* 5'UTR rG4wt and rG4mut region respectively into cells (Figure. 3A) and cells were then fixed with paraformaldehyde and stained by ISCH-adar and FAM-adar probes (Supplementary Table 1). ISCH-adar is composed of a fluorescent light-up moiety specific to G4 structures and an antisense DNA oligo that is complementary to the *ADAR* 5'UTR rG4 flanking sequence (Supplementary Figure. 7). Transfected RNA was localized by the FAM-labeled antisense probe and the FAM signal can be used to eliminate the transfection efficiency variation. We first detected green fluorescence of both *ADAR* 5'UTR rG4wt and rG4mut constructs, confirming the successful transfection of RNA and hybridization with FAM-adar probes in cells (Figure. 3B). The

ISCH-adar red fluorescence can be observed more in the *ADAR* 5'UTR rG4wt region than the *ADAR* 5'UTR rG4mut region, indicating rG4 formation in cells on the *ADAR* 5'UTR rG4wt construct (Figure. 3C). The merge of two fluorescence data displayed a good co-localization in signals (Figure. 3B), highlighting that detected rG4 was from the transfected *ADAR* 5'UTR rG4wt region RNA. RNase control was carried out on cells transfected with *ADAR* 5'UTR rG4wt region, and it exhibited no FAM or ISCH foci (Figure. 3B). This cellular imaging result (Figure. 3) is consistent with the above-mentioned *in vitro* spectroscopic result and structure probing gel (Figure. 1 and Figure. 2), supporting *ADAR* 5'UTR rG4 formation both *in vitro* and in cells.

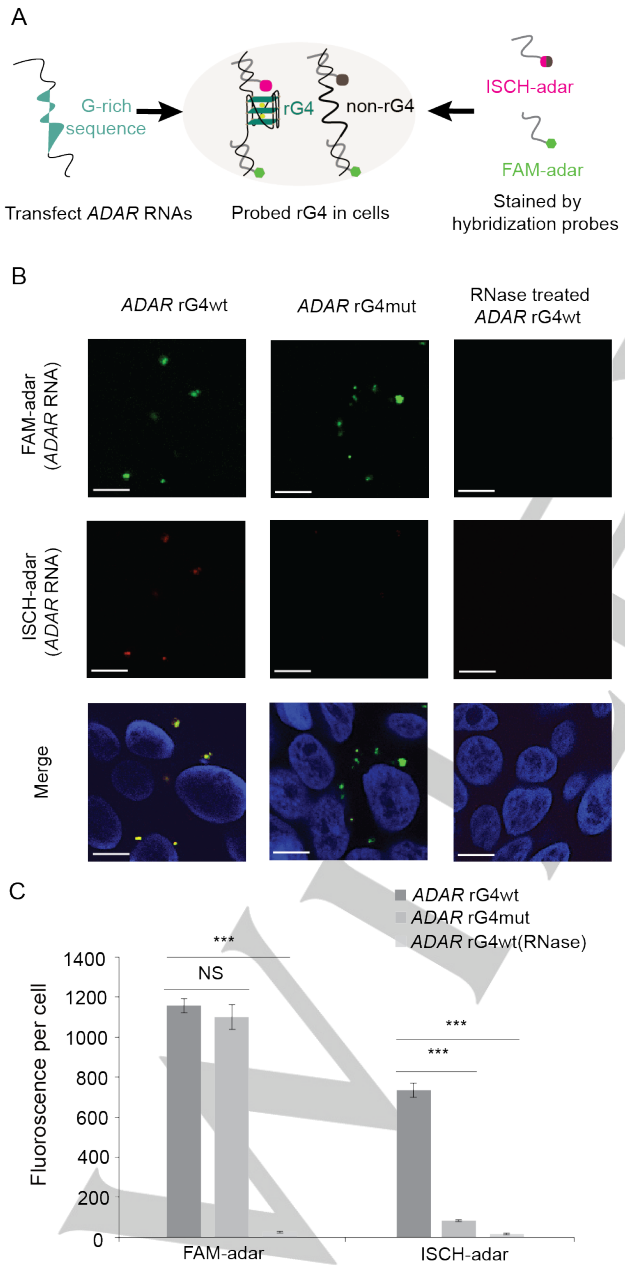

Figure 3. Cell imaging visualizes *ADAR* 5'UTR rG4 formation in cells. (A) Scheme of the hybridized probes targeting flanking sequence for rG4 visualization in cells. *ADAR* 5'UTR RNA was transfected in cells and subsequently, the FAM-adar probe and ISCH-adar probe were incubated for cell staining. (B) Cell imaging of *ADAR* 5'UTR rG4wt and *ADAR* 5'UTR rG4mut region under a confocal microscope detected by FAM-adar probe and ISCH-adar probe. RNase A condition under *ADAR* 5'UTR rG4wt was used as control. Hoechst 33342-stained nuclei are in blue. Scale bar, 10μm. (C) Statistic analysis of ISCH-adar foci and FAM-adar foci in cells. Data were obtained from 300 cells for each sample and three independent experiments were conducted. ***P <0.001, ISCH-adar foci on *ADAR* rG4mut and RNase relative to *ADAR* rG4wt. NS, P >0.05, FAM-adar foci on *ADAR* rG4mut relative to *ADAR* rG4wt. ***P <0.001, FAM-adar foci on RNase relative to *ADAR* rG4wt. P Values were calculated from 3 biological replicates and error bars display the standard error of the mean.

To investigate the *ADAR* 5'UTR rG4 regulatory role in gene expression, we have independently inserted the rG4wt or rG4mut region construct in the 5'UTR of the Renilla luciferase gene sequence, named to be *ADAR* rG4wt and *ADAR* rG4mut DNA plasmid (Supplementary Table 1) and the firefly luciferase gene was used as an internal control to normalize the variation in transfection efficiencies between the rG4wt and rG4mut plasmid. We transfected the plasmids into HEK293T cells, and dual luciferase reporter gene assays were then performed (Figure. 4A). Our results showed that the *ADAR* rG4wt construct has 2.72±0.04-fold lower in normalized luciferase activity comparing with *ADAR* rG4mut construct (Figure. 4B), showing that *ADAR* 5'UTR rG4 plays a down-regulation role in gene expression. To assess whether it is a transcriptional and/or translational effect on gene expression, we also measured the mRNA level by RT-qPCR assay and discovered no significant changes between rG4wt and rG4 mut constructs (Supplementary Figure. 8), supporting that the rG4 acts on translational level.

To verify our result that the translation observed is caused by the effect of rG4 rather than sequence, we treated HEK293T cells with a G4-specific stabilizing ligand, pyridostatin (PDS),[24] to the two constructs mentioned above. Notably, with PDS treatment, the rG4wt construct showed 3.01 ± 0.01-fold lower in luciferase activity when compared with DMSO control, whereas there was no significant difference detected for the rG4mut construct between PDS treatment and DMSO control condition (Figure. 4C and Figure. 4D), illustrating that the PDS effect observed is G4-specific. qPCR assay showed no significant difference across the two constructs when comparing PDS treatment and DMSO control (Supplementary Figure. 9), further supporting the effect of rG4 acting on translation level. We also designed two new vectors, with one containing the full-length *ADAR* 5'UTR (named full 5'UTR rG4wt), and the other with a mutated G-rich sequence (named full 5'UTR rG4mut) (Supplementary Table 1). We performed the reporter gene assays on the two full-length 5'UTR constructs, and consistent results were obtained (Supplementary Figure. 10), which substantiate our results that *ADAR* 5'UTR rG4, in the context of native 5'UTR sequence, has negative regulatory roles in translation.

To further study the *ADAR* 5'UTR rG4 role on the expression of *ADAR* native protein, we designed a new vector containing the

5'UTR and the CDS of *ADAR* native protein and named them to be *ADAR* native_wt and *ADAR* native_mut (Figure. 4E and Supplementary Table 1). To ensure the signal detected is not affected by endogenous *ADAR* protein, we inserted an MYC tag before the stop codon of the two constructs to monitor the MYC-tagged ADAR protein (Figure. 4E).[25] After transfection, we collected cells after 18, 20, 24, 32, 48, and 72h and conducted a western blot assay to detect protein expression level (Figure. 4F and 4G). The *ADAR* native_wt construct showed lower intensity bands on western blot when compared with *ADAR* native_mut in 18, 20, and 24h (approximately 1.42, 1.62, and 1.50-fold), which suggests that rG4 is likely to control the early phase of translation (Figure. 4F and 4G). At 32h and after, the protein expression reaches saturation for both constructs as the band intensity displays slight change, and *ADAR* native_wt showed approximately 2-fold lower expression in comparison with *ADAR* native_mut, indicating that *ADAR* 5'UTR rG4 can control its steady state protein expression (Figure. 4F and 4G). The RT-qPCR result showed that the mRNA level is similar between the two constructs throughout the whole period, indicating that the native gene regulation is on the translational level (Supplementary Figure. 11).

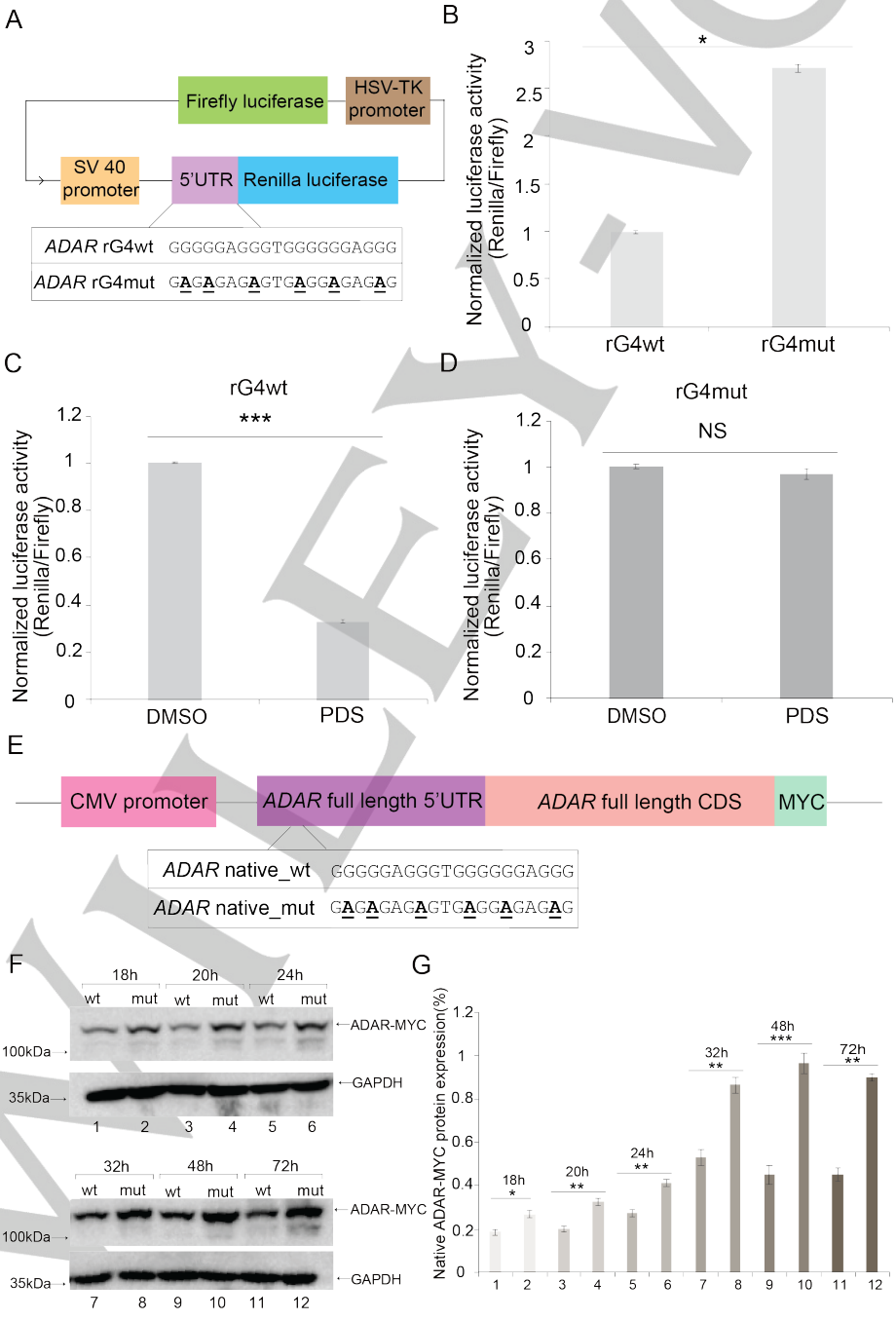

Figure 4. Reporter gene and western blot assay uncover the gene regulatory role of *ADAR* 5'UTR rG4 in cells. (A) The design of reporter gene plasmids. rG4wt or rG4mut sequence is inserted into the 5'UTR of Renilla luciferase gene. (B) Normalized luciferase activity on *ADAR* rG4wt and rG4mut plasmid. Data is the average of normalized luciferase signal two days post-transfection. * *P* <0.05, relative to *ADAR* rG4wt. (C-D) Normalized luciferase activity on *ADAR* rG4wt and rG4mut (left to right) plasmid under 15μM PDS or DMSO. Data is the average of normalized luciferase signal two days post-transfection. *** *P* <0.001, signal under PDS relative to DMSO for *ADAR* rG4wt. NS (not significant), *P* >0.05, signal under PDS relative to DMSO for *ADAR* rG4mut. (E) Scheme of the design of native plasmids. (F-G) Western blot on *ADAR* native_wt and native_mut 18-72h post-transfection. ADAR-MYC is around 110 kDa and GAPDH is around 35 kDa. On the right is the quantification of the western blot result at different time points. * *P* <0.05, native_mut relative to native_wt at 18h. ** *P* <0.01, native_mut relative to native_wt at 20h, 24h, 32h and 72h. *** *P* <0.001, native_mut relative to native_wt at 48h. P Values were calculated from 3 biological replicates and error bars display the standard error of the mean.

DHX36 is a well-studied DEAH family helicase that can bind G4s with strong affinity and resolve G4 in the presence of ATP.[9, 12] Recently, several research groups including ours have reported that DHX36 regulates gene translation through interaction with rG4 in mRNAs in different biological systems.[12-14, 26]To interrogate whether DHX36 can specifically target *ADAR* 5'UTR rG4wt, we conducted an enzyme-linked immunosorbent assay (ELISA) assay on both the *ADAR* 5'UTR rG4wt motif and *ADAR* 5'UTR rG4mut motif under the varying concentration of DHX36 (Figure. 5A). We found that *ADAR* 5'UTR rG4wt motif interacts with DHX36, with a K_d value of 57.04±8.1 nM, confirming strong binding between them. Control experiment using *ADAR* 5'UTR rG4mut showed a much weaker binding (K_d > 200 nM).

Additionally, to study the helicase effect of DHX36 on *ADAR* 5'UTR rG4, we prepared a FAM-labelled *ADAR* wt_unwind construct which contains the *ADAR* 5'UTR rG4 motif and polyA tail to perform the DHX36 unwinding assay (Figure. 5B). *ADAR* wt_Trap DNA sequence is designed to base pair with the *ADAR* wt_unwind construct, and the formation of the duplex can suppress the refolding of rG4 after DHX36 unwinding (Supplementary Table 1). Control experiments were performed to examine the rG4 and duplex formation under varying time, trap DNA concentration, and PEG 8000 conditions, and the results showed that time and PEG 8000 have no observable effect on rG4 – duplex population, whereas trap DNA concentration affects the rG4 – duplex population in a concentration-dependent manner (Supplementary Figure. 12). We incubated the FAM-labelled *ADAR* wt_unwind and *ADAR* wt_Trap DNA alone or together in the presence and absence of DHX36 (Figure. 5C, lanes 1-4). Compared with lane 4, in lane 6 of figure 5C, *ADAR* wt_unwind and *ADAR* wt_Trap DNA formed a stronger duplex band and a lighter rG4 band in the presence of DHX36 and ATP (Figure. 5C). As DHX36 unwinding depends on ATP, we also performed another control experiment (Figure. 5C, lane 5) using a non-hydrolysable ATP analog, AMP-PNP, and the duplex and rG4 band were with similar intensity to lane 4, revealing that ATP is required for the rG4 unwinding reaction, mediated by DHX36. Overall, we illustrated that DHX36 can specifically bind and unwind *ADAR* 5'UTR rG4 *in vitro*.

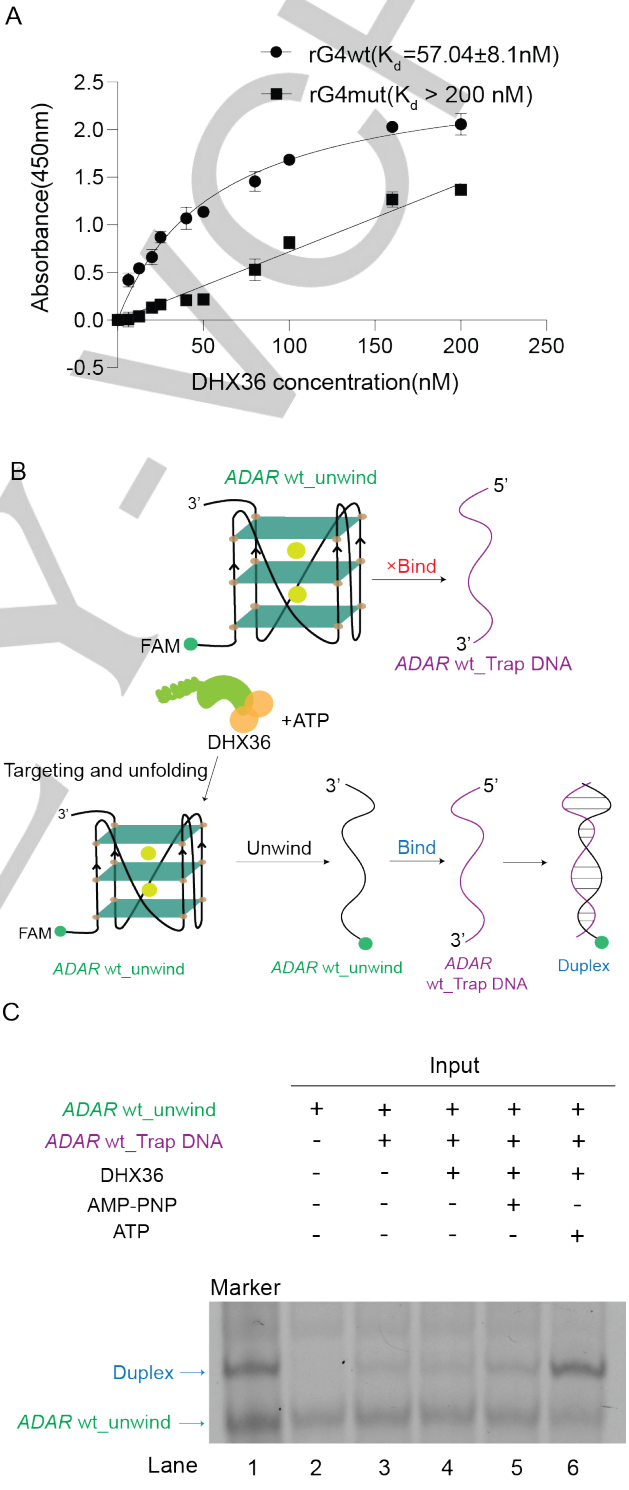

Figure 5. DHX36 targets and unwinds *ADAR* 5'UTR rG4wt *in vitro*. (A) Binding curves and dissociation constants (K_d) determined by ELISA. *ADAR* 5'UTR rG4wt (K_d=57.04±8.1nM) has a high affinity for DHX36, while relatively weaker binding was detected to *ADAR* 5'UTR rG4mut (K_d>200nM). Error bars display the standard error of the mean from three replicates. (B-C) The unwinding assay

scheme and result for DHX36 activity on *ADAR* 5'UTR rG4wt. *ADAR* wt_Trap DNA sequence is fully complementary to the FAM-labeled *ADAR* wt_unwind while the rG4 conformation blocks the duplex formation so that there is a strong rG4 band in lane 3 (C). DHX36 targets and unwinds *ADAR* wt_unwind in an ATP-dependent manner and the resolved *ADAR* wt_unwind can bind to *ADAR* wt_Trap DNA to form a duplex, which causes a shift of band intensity to the duplex conformation (lane 6). AMP-PNP is an analog of ATP that is non-hydrolysable and is used as control (lane 5).

Considering the specificity of DHX36 targeting and resolving activity on *ADAR* 5'UTR rG4 *in vitro*, we wonder if rG4 binding and unwinding by DHX36 can regulate ADAR translation in cells. To test this, we first successfully constructed a DHX36 knockdown (KD) cell line (sh12 cell line) (Supplementary Figure. 13) and performed the reporter gene assay on *ADAR* 5'UTR rG4wt and rG4mut to investigate the effect of DHX36 on these two reporter gene constructs (Supplementary Figure. 14A and B). By comparing sh12 cells to sh3-1 control cells, the *ADAR* 5'UTR rG4wt displayed 1.61 ± 0.01-fold lower luciferase activity signal in DHX36 KD cells, with no significant difference in the mRNA level (Supplementary Figure. 14A and C), suggesting that the gene translation is further repressed in the DHX36 KD cells. In comparison, *ADAR* 5'UTR rG4mut construct on both KD and control cell line display similar levels of luciferase activity signal and mRNA level (Supplementary Figure. 14B and D). It is likely that with the lower DHX36 expression in the KD cell line, the folding state of rG4 was more populated in cells and therefore, reduced the reporter gene translation further. In comparison, as there is no rG4 motif in the *ADAR* 5'UTR rG4mut, no significant difference was observed for this construct in the two cell lines, which supports our hypothesis that DHX36 selectively targets and unwinds rG4.

To further substantiate DHX36's effect on rG4 and gene expression, we constructed a DHX36 knockout (KO) cell line using CRISPR-Cas9 targeting the DHX36 gene with double guide RNAs (Supplementary Table 1). Sequencing and western blotting of the clone confirmed the deletion and loss of DHX36 (Figure. 6A and 6B). We observed the DHX36 unwinding effect on *ADAR* 5'UTR rG4, resulting from the higher ISCH/FAM fluorescence signal ratio in DHX36 KO cells in comparison with the HEK293T cells (Figure. 6C). The normalized ratio indicates the transfected rG4 formation in cells, which meets our hypothesis that there should be more rG4 in folding status without DHX36 in cells. After verification of increased rG4 formation in DHX36 KO cells, we transfected the reporter gene plasmids into KO cells to compare with the HEK293T cells to further examine DHX36's effect on *ADAR* gene regulation. Consistent with the KD results mentioned above, when comparing the result on *ADAR* 5'UTR rG4wt and rG4mut in DHX36 KO and HEK293T cells, the luciferase activity was more repressed (2.92± 0.01-fold) in the KO cells comparing with HEK293T cells on rG4wt, while the difference is not significant in two cell lines on rG4mut (Figure. 6D and 6E). The larger fold (2.92 times) on rG4wt in KO cell lines in comparison with the fold (1.61 times) in KD cell line (Supplementary Figure. 14A) illustrates that knocking out the DHX36 allowed more rG4 population to be in a folded state in cells, which in turn suppressed translation. We also compared the rG4 effect on transcriptional level by differentiating the mRNA level in two cell lines on the two constructs and noticed that there is no significant difference according to the RT-qPCR result on either rG4wt or rG4mut constructs (Supplementary Figure. 15).

To further demonstrate the DHX36's regulatory role in native transcript expression, we also transfected the *ADAR* native_wt into KO and HEK293T cells for comparison (Figure. 6F). As expected, we can see a much lower expression of *ADAR* native_wt in the KO cell line comparing with HEK293T cells. Notably, the ADAR native protein level is significantly reduced throughout the detection process (24h-72h), demonstrating that the rG4 suppression effect is on both gene translation initiation and yield (Figure. 6F). This is consistent with what we have shown in Figure. 4F-G. We also noted that the RT-qPCR result showed that there is less mRNA detected in KO cells compared with HEK293T cells (Supplementary Figure. 16), therefore we cannot rule out the possibility that DHX36 may have some impacts on *ADAR* dG4 formation and transcription. Nevertheless, considering the cell imaging on transfected *ADAR* rG4 constructs, and binding and unwinding between DHX36 and *ADAR* 5'UTR rG4, we have shown clear evidence of the effect of DHX36 on *ADAR* 5'UTR rG4 structure on the reporter and native gene translation. We therefore summarize and propose a model that DHX36 can specifically target and unwind *ADAR* 5'UTR rG4 *in vitro* and in cells, and hence, function as a key regulator in the control of *ADAR* gene expression (Figure. 6G).

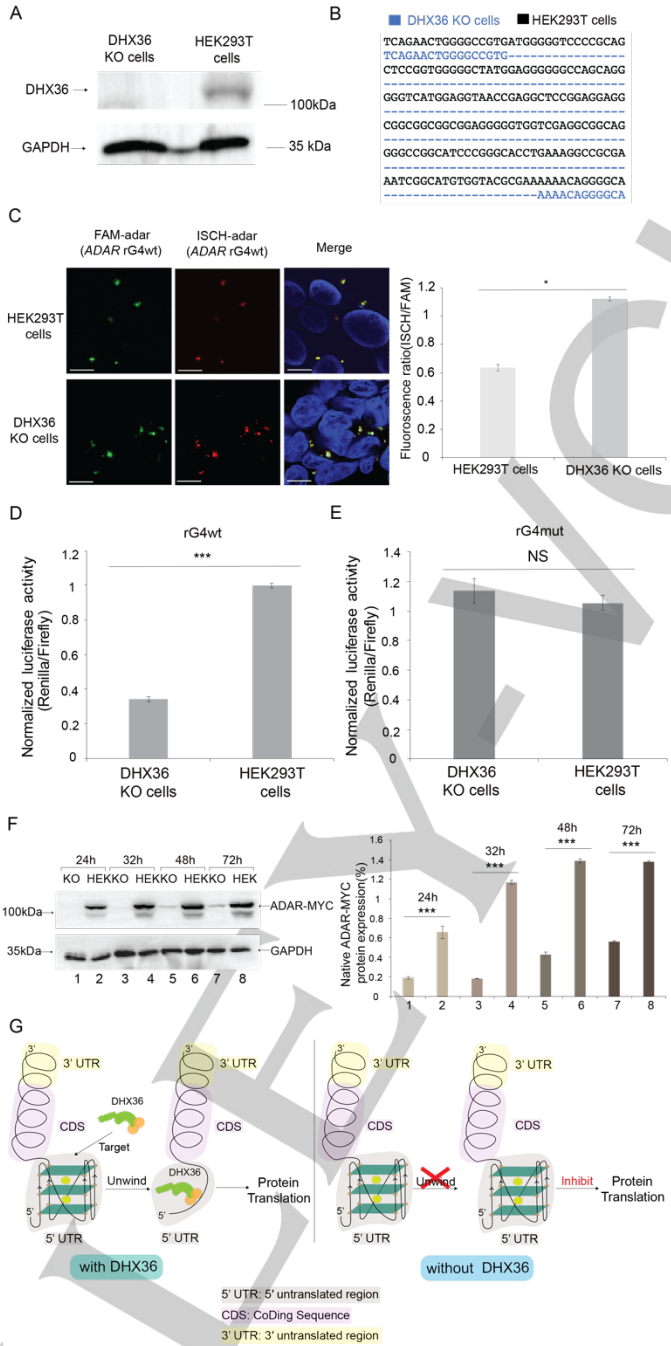

Figure 6. DHX36 regulates translation in an rG4-dependent manner in cells. (A) Deletion of DHX36 was verified by western blot. GAPDH was an internal control. (B) HEK293T cells and DHX36 KO cells sequencing result. The deletion was indicated by dashes. (C) In-cell imaging of transfected *ADAR* 5'UTR rG4wt region with ISCH-adar and FAM-adar probes in HEK293T and KO cells. Scale bar, 10μm. The fluorescence ratio represents the normalization of the ISCH-adar signal to the FAM-adar signal in two cell lines. Hoechst 33342-stained nuclei are in blue. * P <0.05, ISCH/FAM ratio in KO cells relative to HEK293T cells. (D)(E) Normalized luciferase activity on *ADAR* rG4wt (D) and *ADAR* rG4mut (E) in DHX36 KO and HEK293T cells. Data is the average of normalized luciferase signal two days post-transfection. *** P <0.001, *ADAR* rG4wt in KO cells relative to HEK293T cells. NS, P >0.05, *ADAR* rG4mut in KO cells relative to HEK293T cells. (F) Western blot on *ADAR* native_wt 24-72h post-transfection in KO and HEK293T cells. ADAR-MYC is around 110 kDa and GAPDH is around 35 kDa. Right is the quantification of western blot at different time points. *** P <0.001, KO relative to HEK293T cells at all time points. P Values were calculated from 3 biological replicates and error bars display the standard error of the mean. (G) Schematic illustration of the mechanism of DHX36 modulating protein translation in an rG4-dependent manner.

In this study, we report the formation of a thermostable 5'UTR rG4 structure on the *ADAR1* transcript, reveal DHX36 to bind and unwind *ADAR1* 5'UTR rG4, and uncover the effect and interplay of rG4 and DHX36 on *ADAR1* translation. Below we highlight the approaches employed and insights obtained from this work and compare them with other 5'UTR rG4 and DHX36 works in the literature.

Transcriptome-wide rG4 mapping using rG4-seq has provided the G4 and RNA community with a repertoire of experimentally detected rG4 candidates that can be readily used for further structural and functional investigation on a transcript-specific basis.[21] Compared to other 5'UTR rG4 studies,[1a, 4a] the rG4s in those earlier works, such as *NRAS*,[5b] *MT3-MMP*,[4b], and *Zic-1*,[6b] were initially predicted using computational algorithms based on

a consensus sequence motif, which then was later confirmed by additional experiments. These different approaches are complementary to each other. Using the rG4-seq dataset,[21] we have successfully identified an rG4 located at the 5'UTR of *ADAR1* transcript, and we further characterized the rG4 structure and folding both *in vitro* and in cells using an extensive set of techniques (Figure. 1-3). While CD (Supplementary Figure.1), UV melting (Supplementary Figure. 2), and G4 ligand-enhanced fluorescence (Figure. 1) are the gold standard assays for rG4 detection,[2a] we have also applied relatively new and important assays, such as RTS, SHALiPE, and cell imaging using GTFH probes.[22-23, 27] Using RTS and SHALiPE assays (Figure. 2), we were able to provide a higher resolution view of the *ADAR1* 5'UTR rG4 in the context of flanking regions as compared to the spectroscopic assays mentioned above, with the RTS assay result largely consistent with the published rG4-seq data. By using SHALiPE, we can also understand the rG4 folding status in cell lysate (Supplementary Figure.6). Due to the long runs of Gs in this *ADAR1* 5'UTR rG4 motif, i.e., G5-G3-G6-G3 tracts, we were not able to resolve and propose the secondary structure, as it is likely that multiple rG4 conformations co-existed based on the structure probing data. However, the presence of multiple rG4 conformations did not seem to impact their overall cellular folding status, as cell imaging data using the GTFH probes provided a clear and strong signal for rG4 formation in cells (Figure. 3). Noteworthy, the rG4 polymorphism exhibited by this *ADAR1* 5'UTR rG4 motif suggested many rG4 structures are to be expected, and each of them may have minor difference in structure features that can potentially influence its thermostability, its binding recognition with DHX36, and its ability to be resolved by DHX36. In this *ADAR1* 5'UTR rG4 motif, we speculate that instead of a "digital" molecular switch (on/off), its rG4 polymorphism may contribute to a more "analog" molecular rheostat (tunable) gene regulation and control. Future experiments will be needed to gain in-depth structural and molecular insights into this specific rG4 motif. Collectively, these spectroscopic, structural probing, and imaging assays provide substantial corroboration in determining both the structural features of rG4, as well as the folding status of rG4 in cells.

Using a dual luciferase reporter gene system, our data suggested that *ADAR* 5'UTR rG4 is responsible for the downregulation of gene translation in cells (Figure. 4B), which is consistent with many 5'UTR rG4 studies that also used reporter gene assay.[4a, 4b, 6b, 28] The approximately 3-fold effect on translational suppression in *ADAR* 5'UTR rG4 is similar to other 5'UTR rG4s reported.[4a] To extend our study and understanding, we further explored this initial discovery in 3 major ways. First, we investigated the effect of *ADAR* 5'UTR rG4 on the construct that contained *ADAR* native protein with an MYC tag and performed western blot analysis at different time points (Figure. 4F). Our data suggested that rG4 can control the early phase of translation as well as the steady state protein expression level. Second, we identified DHX36 as an *ADAR* 5'UTR rG4 binder, which can interact and unwind *ADAR* 5'UTR rG4 specifically (Figure. 5). Notably, we constructed DHX36 KO cell lines using CRISPR-Cas9 (Figure. 6A and B) and showed that both the rG4 foci in the imaging assays and the luciferase activity in reporter gene assay for *ADAR* 5'UTR rG4 increased in the absence of DHX36 (Figure. 6C and D), highlighting the interplay of *ADAR* 5'UTR rG4 and DHX36 in cells. Last, we also compared the native gene expression quantity in DHX36 KO cells and HEK293T cells at different time points (Figure. 6F) and found that lower ADAR-MYC protein expression was observed in DHX36 KO cells, indicating that the absence of DHX36 is likely to allow more rG4s folded in cells, which in turn inhibits the protein production. We cannot eliminate the possibility that dG4 may also have a role in this result, as we also observed that the mRNA level of *ADAR* native_wt was lower in KO cells compared with HEK293T cells (Supplementary Figure. 16), illustrating that DHX36 KO might also affect dG4 folding in cells, and cause transcriptional regulation. Nevertheless, our imaging and reporter gene data clearly illustrate that rG4 and DHX36 have significant roles in this *ADAR1* gene translation (Figure. 6G).

The approaches and the resultant findings reported in this work are original and provide fundamental insights for further investigation of *ADAR1* 5'UTR rG4 and DHX36 in other cellular conditions and systems in the future. ADAR1 plays a specific role in RNA editing for the changes in editing the double-stranded transcripts with specific A to I mutation and inhibition of ADAR1 remarkably reduces tumor growth[20]. We here propose the *ADAR1* 5'UTR rG4 to be a significant regulator of *ADAR1* translation. From previous 5'UTR rG4 studies, it was suggested that rG4 on the 5'UTR could hinder the recruitment of pre-initiation complex at the beginning of translation or block the ribosome small subunit from the scanning of the start codon of mRNA,[29] and *ADAR1* 5'UTR rG4 likely coordinates with DHX36 and potentially other unidentified binding proteins to control gene translation. The future structural and functional study will delineate the detailed molecular mechanism in full. This will facilitate the development of targeting tools towards *ADAR1* 5'UTR rG4, DHX36, and other associated proteins, which can be accustomed to potentially control gene expression and RNA editing through the regulation of *ADAR1*.

Conclusion

In sum, we identified and characterized the *ADAR* 5'UTR rG4 formation both *in vitro* and in cells for the first time. Subsequently, we comprehensively studied the repressive role of *ADAR* 5'UTR rG4 on gene expression in cells through reporter gene assay and native protein analysis. We also revealed the interaction of *ADAR* 5'UTR rG4 with DHX36 and demonstrated DHX36's regulatory role on *ADAR* gene expression through the unwinding of *ADAR* 5'UTR rG4 in cells. We also developed and applied rG4 imaging assays to monitor *ADAR* 5'UTR rG4 folding status in HEK293T and DHX36 CRISPR-Cas9 KO cells to support the results from spectroscopic, structural, and functional assays. The strategies and findings presented here enable the further characterization and functional study of rG4s in other regions of mRNA, as well as in different classes of non-coding RNA.

Acknowledgments

We thank Dr. Xiaona Chen and Prof. Huating Wang for their assistance and discussion. Research Grants Council of the Hong Kong SAR, China Projects [CityU 11100222, CityU 11100421, CityU 11101519, CityU 11100218, N_CityU110/17]; National Natural Science Foundation of China Project [32222089]; Croucher Foundation Project [9509003]; State Key Laboratory of Marine Pollution Director Discretionary Fund; City University of Hong Kong projects [7005503, 9667222, 9680261] to C.K.K. The National Natural Science Foundation of China (No. 21977124, 81973184) to the Tan laboratory. CUHK Direct Grant [4053486]; Hong Kong Research Grants Council Area of Excellence Scheme [AoE/M-403/16]; the Innovation and Technology Commission, Hong Kong SAR (State Key Laboratory of Agrobiotechnology, CUHK) to T.F.C.; Hong Kong Ph.D. Fellowship Scheme to E.Y.C.C.; The grants from Tung Biomedical Sciences Center to J.S.

Keywords: RNA G-quadruplex • ADAR • DHX36 • gene expression • structure-function relationship

Conflict of interest

The authors declare no conflict of interest.

[1] a)K. Lyu, E. Y. Chow, X. Mou, T. F. Chan, C. K. Kwok, *Nucleic Acids Res* **2021**, *49*, 5426-5450; b)L. Dumas, P. Herviou, E. Dassi, A. Cammas, S. Millevoi, *Trends Biochem Sci* **2021**, *46*, 270-283; c)L. R. Ganser, M. L. Kelly, D. Herschlag, H. M. Al-Hashimi, *Nat Rev Mol Cell Biol* **2019**, *20*, 474-489.

[2] a)C. K. Kwok, C. J. Merrick, *Trends Biotechnol* **2017**, *35*, 997-1013; b)C. K. Kwok, G. Marsico, S. Balasubramanian, *Cold Spring Harb Perspect Biol* **2018**, *10*, a032284; c)S. B. S. Neidle, in *Quadruplex Nucleic Acids* (Eds.: S. Neidle, S. Balasubramanian), The Royal Society of Chemistry, **2006**, pp. 100-130.

[3] S. Millevoi, H. Moine, S. Vagner, *Wiley Interdiscip Rev RNA* **2012**, *3*, 495-507.

[4] a)A. Bugaut, S. Balasubramanian, *Nucleic Acids Res* **2012**, *40*, 4727-4741; b)M. J. Morris, S. Basu, *Biochemistry* **2009**, *48*, 5313-5319; c)M. Wieland, J. S. Hartig, *Chem Biol* **2007**, *14*, 757-763.

[5] a)C. Schaeffer, B. Bardoni, J. L. Mandel, B. Ehresmann, C. Ehresmann, H. Moine, *EMBO J* **2001**, *20*, 4803-4813; b)S. Kumari, A. Bugaut, J. L. Huppert, S. Balasubramanian, *Nat Chem Biol* **2007**, *3*, 218-221.

[6] a)R. Jodoin, L. Bauer, J. M. Garant, A. Mahdi Laaref, F. Phaneuf, J. P. Perreault, *RNA* **2014**, *20*, 1129-1141; b)A. Arora, M. Dutkiewicz, V. Scaria, M. Hariharan, S. Maiti, J. Kurreck, *RNA* **2008**, *14*, 1290-1296; c)C. K. Kwok, Y. Ding, S. Shahid, S. M. Assmann, P. C. Bevilacqua, *Biochem J* **2015**, *467*, 91-102; d)H. Cho, H. S. Cho, H. Nam, H. Jo, J. Yoon, C. Park, T. V. T. Dang, E. Kim, J. Jeong, S. Park, E. S. Wallner, H. Youn, J. Park, J. Jeon, H. Ryu, T. Greb, K. Choi, Y. Lee, S. K. Jang, C. Ban, I. Hwang, *Nat Plants* **2018**, *4*, 376-390.

[7] a)M. C. Chen, R. Tippana, N. A. Demeshkina, P. Murat, S. Balasubramanian, S. Myong, A. R. Ferre-D'Amare, *Nature* **2018**, *558*, 465-469; b)E. K. S. McRae, E. P. Booy, A. Moya-Torres, P. Ezzati, J. Stetefeld, S. A. McKenna, *Nucleic Acids Res* **2017**, *45*, 6656-6668; c)T. Santos, A. Miranda, M. P. C. Campello, A. Paulo, G. Salgado, E. J. Cabrita, C. Cruz, *Biochem Pharmacol* **2021**, *189*, 114208; d)J. A. Imperatore, D. S. McAninch, A. N. Valdez-Sinon, G. J. Bassell, M. R. Mihailescu, *Front Mol Biosci* **2020**, *7*, 6; e)R. Goering, L. I. Hudish, B. B. Guzman, N. Raj, G. J. Bassell, H. A. Russ, D. Dominguez, J. M. Taliaferro, *Elife* **2020**, *9*, e52621.

[8] R. Tippana, M. C. Chen, N. A. Demeshkina, A. R. Ferre-D'Amare, S. Myong, *Nat Commun* **2019**, *10*, 1855.

[9] J. P. Vaughn, S. D. Creacy, E. D. Routh, C. Joyner-Butt, G. S. Jenkins, S. Pauli, Y. Nagamine, S. A. Akman, *J Biol Chem* **2005**, *280*, 38117-38120.

[10] S. D. Creacy, E. D. Routh, F. Iwamoto, Y. Nagamine, S. A. Akman, J. P. Vaughn, *J Biol Chem* **2008**, *283*, 34626-34634.

[11] A. N. Sexton, K. Collins, *Mol Cell Biol* **2011**, *31*, 736-743.

[12] M. Sauer, S. A. Juranek, J. Marks, A. De Magis, H. G. Kazemier, D. Hilbig, D. Benhalevy, X. Wang, M. Hafner, K. Paeschke, *Nat Commun* **2019**, *10*, 2421.

[13] X. Chen, J. Yuan, G. Xue, S. Campanario, D. Wang, W. Wang, X. Mou, S. W. Liew, M. I. Umar, J. Isern, Y. Zhao, L. He, Y. Li, C. J. Mann, X. Yu, L. Wang, E. Perdiguero, W. Chen, Y. Xue, Y. Nagamine, C. K. Kwok, H. Sun, P. Munoz-Canoves, H. Wang, *Nat Commun* **2021**, *12*, 5043.

[14] J. Nie, M. Jiang, X. Zhang, H. Tang, H. Jin, X. Huang, B. Yuan, C. Zhang, J. C. Lai, Y. Nagamine, D. Pan, W. Wang, Z. Yang, *Cell Rep* **2015**, *13*, 723-732.

[15] a)L. P. Keegan, A. Leroy, D. Sproul, M. A. O'Connell, *Genome Biol* **2004**, *5*, 209; b)K. Nishikura, *Annu Rev Biochem* **2010**, *79*, 321-349; c)B. L. Bass, *Annu Rev Biochem* **2002**, *71*, 817-846; d)A. M. Chalk, S. Taylor, J. E. Heraud-Farlow, C. R. Walkley, *Genome Biol* **2019**, *20*, 268.

[16] M. Heep, P. Mach, P. Reautschnig, J. Wettengel, T. Stafforst, *Genes (Basel)* **2017**, *8*, 34.

[17] T. Merkle, S. Merz, P. Reautschnig, A. Blaha, Q. Li, P. Vogel, J. Wettengel, J. B. Li, T. Stafforst, *Nat Biotechnol* **2019**, *37*, 133-138.

[18] a)J. Galipon, R. Ishii, Y. Suzuki, M. Tomita, K. Ui-Tei, *Genes (Basel)* **2017**, *8*, 68; b)H. A. Hundley, B. L. Bass, *Trends Biochem Sci* **2010**, *35*, 377-383.

[19] E. Picardi, C. Manzari, F. Mastropasqua, I. Aiello, A. M. D'Erchia, G. Pesole, *Sci Rep* **2015**, *5*, 14941.
[20] T. Sun, Y. Yu, X. Wu, A. Acevedo, J. D. Luo, J. Wang, W. M. Schneider, B. Hurwitz, B. R. Rosenberg, H. Chung, C. M. Rice, *Proc Natl Acad Sci U S A* **2021**, *118*, e2021757118.
[21] C. K. Kwok, G. Marsico, A. B. Sahakyan, V. S. Chambers, S. Balasubramanian, *Nat Methods* **2016**, *13*, 841-844.
[22] C. K. Kwok, S. Balasubramanian, *Angew Chem Int Ed Engl* **2015**, *54*, 6751-6754.
[23] C. K. Kwok, A. B. Sahakyan, S. Balasubramanian, *Angew Chem Int Ed Engl* **2016**, *55*, 8958-8961.
[24] A. De Magis, S. G. Manzo, M. Russo, J. Marinello, R. Morigi, O. Sordet, G. Capranico, *Proc Natl Acad Sci U S A* **2019**, *116*, 816-825.
[25] E. Crenshaw, B. P. Leung, C. K. Kwok, M. Sharoni, K. Olson, N. P. Sebastian, S. Ansaloni, R. Schweitzer-Stenner, M. R. Akins, P. C. Bevilacqua, A. J. Saunders, *PLoS One* **2015**, *10*, e0143160.
[26] a)P. Murat, G. Marsico, B. Herdy, A. T. Ghanbarian, G. Portella, S. Balasubramanian, *Genome Biol* **2018**, *19*, 229; b)C. J. Maltby, J. P. R. Schofield, S. D. Houghton, I. O'Kelly, M. Vargas-Caballero, K. Deinhardt, M. J. Coldwell, *Nucleic Acids Res* **2020**, *48*, 9822-9839.
[27] S. B. Chen, M. H. Hu, G. C. Liu, J. Wang, T. M. Ou, L. Q. Gu, Z. S. Huang, J. H. Tan, *J Am Chem Soc* **2016**, *138*, 10382-10385.
[28] D. Gomez, A. Guedin, J. L. Mergny, B. Salles, J. F. Riou, M. P. Teulade-Fichou, P. Calsou, *Nucleic Acids Res* **2010**, *38*, 7187-7198.
[29] a)A. L. Wolfe, K. Singh, Y. Zhong, P. Drewe, V. K. Rajasekhar, V. R. Sanghvi, K. J. Mavrakis, M. Jiang, J. E. Roderick, J. Van der Meulen, J. H. Schatz, C. M. Rodrigo, C. Zhao, P. Rondou, E. de Stanchina, J. Teruya-Feldstein, M. A. Kelliher, F. Speleman, J. A. Porco, Jr., J. Pelletier, G. Ratsch, H. G. Wendel, *Nature* **2014**, *513*, 65-70; b)M. Kozak, *Proc Natl Acad Sci U S A* **1986**, *83*, 2850-2854; c)M. Kozak, *Mol Cell Biol* **1989**, *9*, 5134-5142; d)J. R. Babendure, J. L. Babendure, J. H. Ding, R. Y. Tsien, *RNA* **2006**, *12*, 851-861; e)A. E. Koromilas, A. Lazaris-Karatzas, N. Sonenberg, *Embo j* **1992**, *11*, 4153-4158.

Table of Contents

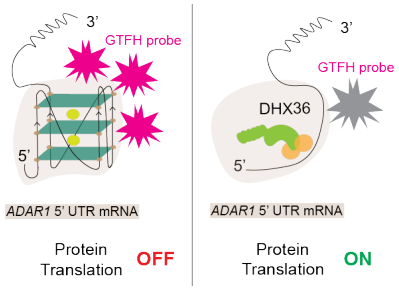

An RNA G-quadruplex (rG4) structure was identified in the 5'UTR of the *ADAR1* mRNA using multi-disciplinary assays *in vitro* and cells. The binding and resolving effect of rG4-specific helicase DHX36 on this rG4 was monitored using G-quadruplex-triggered fluorogenic hybridization (GTFH) probe. Functionally, *ADAR1* 5'UTR rG4 inhibits reporter gene and native transcript translation with DHX36 modulating its formation in cells.

Institute and/or researcher Twitter usernames: @kitkwok6, @cityuchem, @cityuscience